ELSEVIER

Physica B 271 (1999) 386–395

PHYSICA B

www.elsevier.com/locate/physb

Pseudo hysteresis current loop and negative differential resistance in cluster superlattice of tellurium in zeolite

X.R. Wang*, Z.K. Tang, W.K. Ge

Physics Department, The Hong Kong University of Science and Technology, Clear Water Bay, Hong Kong

Received 3 December 1998

Abstract

We study electron transport properties of tellurium (Te) cluster superlattice in Linde type-A zeolite. Applying a constant voltage, current–voltage (I–V) curve shows a hysteresis loop with a pseudo negative differential resistance (PNDA). The current loop and the current peak are history dependent. Under the same experimental conditions, we find that the current peak position moves to a higher voltage when the sample temperature is increased. Applying a variable voltage, I–V curve can be both monotonic and non-monotonic, depending on the frequency of the source. If a biased source is applied on the sample, the I–V curve will change with time, and eventually reach a stable state at which the current is a monotonical function of voltage. We clarify that both the current loop and peak are transient phenomena. The main transport mechanism is identified as non-resonant electron tunneling. The observed I–V characteristics can be attributed to the structure change of Te clusters inside the zeolite cages under an external electric field. The current peak can be understood as the effect of the finite transient time during which the Te cluster structure changes from one to another under an applied voltage. The temperature dependence of the peak position can be well described by many small collision assumption. With a simple mean-field-type approximation, the peak position is found to be proportional to the square root of the temperature. © 1999 Elsevier Science B.V. All rights reserved.

PACS: 73.61. – r; 81.05.Zx; 73.40.Gk

Keywords: Superlattice; Tunneling; Zeolite

1. Introduction

There has been great interest in studying electron transport of quantum dot arrays, semiconductor superlattices, and cluster and molecular solids (superlattices) in recent decades. Firstly, growth techniques such as molecular beam epitaxy(MBE) and metal–organic chemical vapor deposition (MOCVD) make it possible to realize artificial periodic structures, thus one can get a hand on the material properties through band structure engineering. Secondly, nanoparticles, superlattices and quantum wells show many interesting properties in terms of response time and transport efficiency [1]. In general, the properties of superlattices reflect both the properties of individual building cells and extended systems [2]. Many devices based on novel properties of these systems have been proposed and made [3]. A spectacular electrical

---

* Corresponding author. Tel.: + 852-2358-7488; fax: + 852-2358-1652.

E-mail address: phxwan@usthk.ust.hk (X.R. Wang)

PII: S0921-4526(99)00200-8

characteristic observed in a double-barriered quantum well is the phenomenon of negative differential resistance (NDR) resulting from the resonant electron tunneling [4,5]. A series of such NDR regions have been observed in superlattice structures due to the sequential resonant tunneling through quantum wells [6]. Any fluctuation in the well structures or non-uniformities in the electric field, however, will destroy the sequential tunneling in a superlattice system. Besides the superlattices made by MBE and MOCVD, zeolites with a regular network of pores which can be filled with various substances are a new form of solids. Such cluster superlattices have drawn considerable attention in recent years [7]. A zeolite-based cluster superlattice offers a good ground for studying the electron transport among small clusters that are arranged in spatially three-dimensional arrays. Since the basic building unit is a cluster which consists of tens of atoms, such cluster superlattices have a number of interesting properties which have not yet been detected for ordinary crystals [8,9].

Bogomolov et al. [8] studied the current–voltage (I–V) characteristics of tellurium (Te) clusters in cavities of zeolite X (faujasite). The Te clusters are connected one with another when zeolite NiNaX is used as the matrix, where some of the Na^+ in the cavity walls is replaced by Ni^{2+}. The Te clusters are well separated from each other with a weak interaction between them when zeolite NaX is used as the matrix. In the first case they found that the I–V characteristic has a series of S-shaped regions. They claimed that the behavior is due to the breakdown between the minizones of tellurium under the influence of volume modulation of the zeolite matrix. In the second case, the I–V characteristic shows a series of successive current surges as the field increases. They explained the observation as the resonance tunneling between the energy levels of the clusters in neighboring cavities. Recently, we studied the I–V characteristic of Te cluster superlattice in Linde type-A zeolite (Te/LTA). We thought that the electron–electron interaction should be strong in Te/LTA solids (cluster superlattices) since there are as many as 16 Te atoms in each cluster of the size about 11 Å. Therefore, our initial motivation is to use the system to study the Coulomb interaction effects. Surprisingly, we observed hysteresis current loops and current peaks in the I–V characteristics [9]. We found that the current loops and peaks depend on the sample temperature, the duration time of the applied voltage, the frequency of the AC source, etc. We attribute the current peaks (pseudo negative differential resistance (NDR)) to the rearrangement of Te atoms in the cluster. In this paper, we give a detailed analysis of the experimental results, and demonstrate theoretically that the observed phenomena can be explained by the structure changes of Te clusters under an external electric field. In Section 2, we describe our sample preparation, experimental procedure and results. In Section 3, we will argue that the transport mechanism is mainly the quantum tunneling of an electron through the potential barrier between clusters. Under the assumption that the observed phenomena are due to the structure change of Te clusters, we estimate the transient time and temperature dependence of the peak positions. With plausible parameters for the material, the estimations agree well with the experimental data. Summary and conclusions are presented in Section 4.

2. Experimental methods

Linde-type-A (LTA) zeolite is constructed by linking AlO_4^- and SiO_4 tetrahedra together with shared oxygen atoms. It contains cations Na^+ and anions AlO_4^-. The chemical formula of LTA is given by $Na_{12}Al_{12}Si_{12}O_{48}$. The frame work of LTA consists of sodalite cages and supercages with inside diameters of about 6 and 11 Å, respectively. Supercages are interconnected in a simple cubic structure by sharing windows of 4 Å diameter. The center distance between two neighboring supercages is 12.3 Å. There is a thin barrier (~ 1.3 Å) between the clusters. Fig. 1 shows schematically the unit framework of zeolite LTA. Most of Na^+ ions exist inside the sodalite cages, near the 6-rings faced to the supercages. It has been known [10–12] that adsorption ability of a zeolite is determined by the dipole field of these metal cations and AlO_4^- anions. De Lara et al. [12] had studied electric-field effect on molecule adsorption in zeolite LTA. They showed that there is a very strong internal electric field near the cage surface.

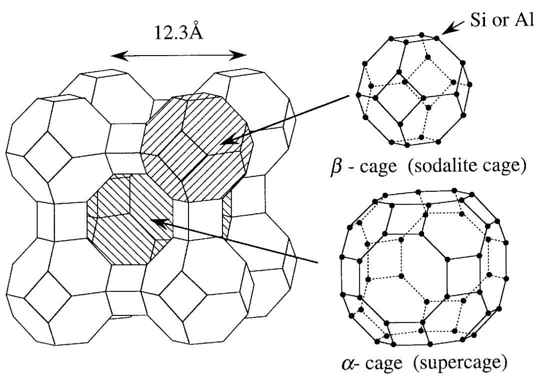

Fig. 1. Structure of zeolite LTA. Na^+ ions exist near the 6-ring in sodalite cage side, facing the supercage. The dipole field of AlO_4^-–Na^+ points outward. Te clusters with size of 11 Å in diameter are arranged in a simple cubic structure with lattice constant of 12.3 Å. There is a thin barrier (~ 1.3 Å) between the clusters.

2.1. Sample preparation

The Na-type LTA crystals were grown by reacting sodium metasilicate with sodium aluminate, using triethanolamine as a stabilizing and buffering agent. After filtered through a 0.2 mm pore size filter, the aluminate solution was stirred into the silicate solution in a jar, covered, and placed in an electric oven at 80°C for 2–3 weeks. The typical crystal size is about 30 μm. By adding some seeds into the growth solution, large crystals of about 100 μm can be obtained. But most of them are polycrystals because of the random growth on the seed surface. Single crystals selected out from the products were used in the experiments. The LTA single crystals were dehydrated by heating in a glass ampoule in vacuum up to 550°C for 4 h, and were then sealed together with Te source (99.999% purity). The sealed ampoule was heated uniformly at 250°C for 48 h and cooled to room temperature gradually. The original LTA crystal is transparent. It changes into light brown in color after absorbing Te atoms. The electrical characteristics were measured by clamping the single crystal between a tungsten needle and an indium electrode on a hot plate which can heat the sample. The *I–V* properties were measured using a Keithley Source-Measure Unit (Model 236). For the measurement of frequency dependence, a Stanford Function Generator (Model DS335) was used as the voltage source.

2.2. Experimental results

Fig. 2 shows the current–voltage characteristics of a Te/LTA sample at 295 K. The current peak in curve (a) looks like the resonant tunneling transitions as observed in a double-barriered quantum well [5]. However, the loops and the peaks are history dependent. Curve (a) is the *I–V* characteristic of an as-fabricated sample. Under forward bias, the current peak is seen near 2.4 V. Under reverse bias, however, the current does not return along the trace of the forward bias, but decreases with the decrease in the bias, hence forming a loop with a bias circle. Repeating the same measurement soon after (a), the current peak is found to be broadened while the loop area decreases, as shown

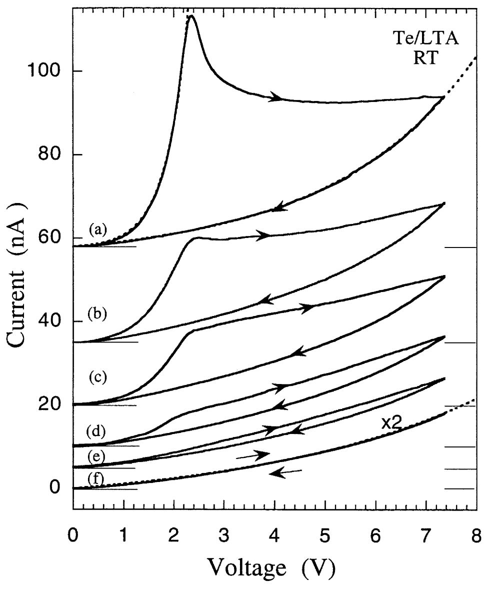

Fig. 2. *I–V* characteristics at room temperature (295 K) when a constant voltage source is used. The voltage is changed every half-second by 0.05 V. (a) *I–V* characteristic of the first round measurement. The current first increases until it peaks near 2.4 V. (b), (c), (d) and (e) are the second, third, fourth and fifth round measurements, respectively. (f) is the current measured after the sample was "annealed" under 20 V voltage bias for 1 h. It can be fitted well by Eq. (5) (dashed line) with $\alpha = 0.15$.

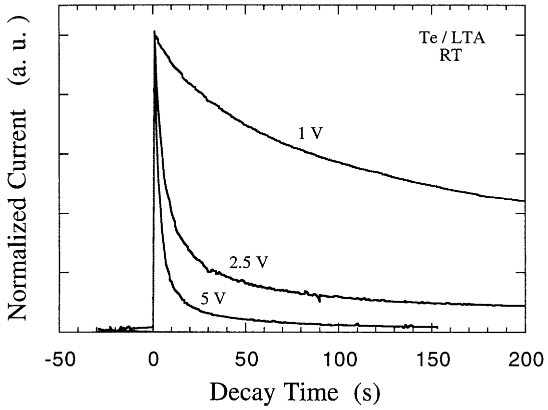

Fig. 3. The time dependence of the current under a constant applied bias of 1, 2.5, and 5 V, respectively.

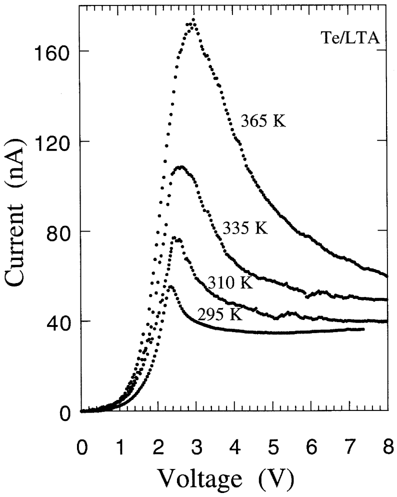

Fig. 4. I–V curves measured at 295, 310, 335 and 365 K, respectively. Before each measurement, the sample is in its nature state (Te atoms adsorbed on the inner surface of supercages).

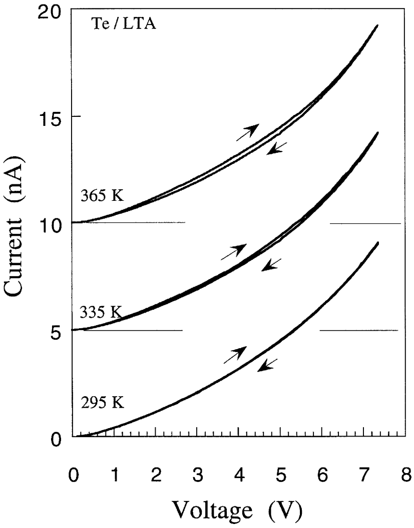

Fig. 5. I–V curves at 295, 335 and 365 K, respectively, when the current is almost in its stable state (after an unsymmetric bias is applied to the system for a long time).

in curve (b). One round measurement takes about 30 min. When the measurement is repeated again and again, the loop area becomes smaller and smaller, as shown in curves (c)–(e). Curve (f) is the current measured after the sample was "annealed" under a constant bias of 20 V for 1 h, in which the loop disappears, that implies that the system becomes stable. Those return curves and curve (f) can be fitted well by Eq. (5). The dash lines in curves (a) and (f) in Fig. 2 are the fit to Eq. (5). The values of the exponent α are 0.23 and 0.15, respectively. We would like to take this opportunity to revise our estimated values of α (α were estimated to be 0.35 and 0.09 in our previous publication, Ref. [9]). We had used a simple exponential function, rather than Eq. (5), to estimate the value of α in Ref. [9]. Unfortunately, the simple exponential function cannot be a correct expression for the I–V curve because it will not lead to the correct limit of $I = 0$ as $V \to 0$. If the sample is heated up to a high temperature, or an external voltage in opposite direction is applied to the sample before one measures the sample again, curves (a)–(f) can be reproduced. In addition to the current loop behavior, the current is found to decay even under a constant applied bias. Fig. 3 shows the current decay measured by keeping a voltage bias of 1, 2.5, and 5 V, respectively, on an as-fabricated sample. Under small bias, say 1 V, the current decay is very slow. It takes a few 10 min before the current approaches a constant value. The decay speed increases as the applied bias increases. The current peak in curve (a) of Fig. 2 depends on temperature. Fig. 4 is the I–V curves measured at 295, 310, 335 and 365 K, respectively. It is clear that the peak moves to a higher voltage when the sample temperature increases. However, curve (f) is not very sensitive to temperature. Fig. 5

is the stable I–V curves measured at 295, 335 and 365 K. In order to have a deep insight into the origin of the current loops and peaks of curve (a) in Fig. 2, we measured the I–V curves by applying a triangular voltage wave. Under low-frequency bias of 100 Hz, as shown in Fig. 6(a), the I–V curve is a non-monotonic function of voltage, showing a negative differential resistance region. When the frequency increases to 10 kHz, as shown in Fig. 6(b), a very symmetrical current wave is detected.

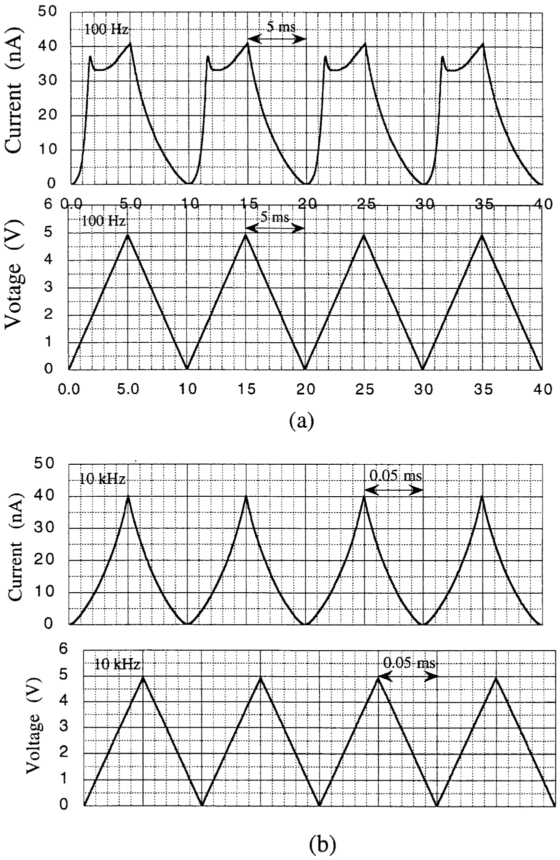

Fig. 6. AC I–V curves measured at room temperature (295 K). The AC voltage source is a triangular wave. The frequency in (a) is 100 Hz and that in (b) is 10 kHz.

3. Theoretical methods

3.1. Electron transport mechanism

In order to understand the above anomalous I–V characteristics of the Te/LTA cluster superlattices, we should first find out the electron transport mechanism. The Te clusters in LTA supercages are spatially confined. An electron needs to overcome a potential barrier when it moves from one cluster to another. The overlap of electronic states in two nearest Te clusters should be small. Therefore, there are two possible processes dominating the electron conduction in this system. Electrons can either be thermally excited and hop over the potential barrier between the two clusters, or quantum mechanically tunnel through the barrier. Thermally activated hopping probability is proportional to the exponential of the inverse of the temperature and to the potential barrier height. This probability is small for a large potential barrier. It is known that the thermally activated hopping process is important for thick barriers and the quantum tunneling process should dominate when the potential barrier is high but thin [4]. In our case, the distance between the two nearest-neighbor clusters is only 1.3 Å (thin barrier) and the potential barrier is expected to be high (order of eV). Thus, the quantum tunneling process is expected to dominate the electron transport in the system. This assumption agrees with the experimental fact that the stable I–V characteristics is not sensitive to temperature as shown in Fig. 5. The quantum tunneling current under a biased voltage, eV, between a potential barrier is given by

$$I = \frac{2e}{h}\sum_{k}\int_{E_{\perp}} P[f(E) - f(E + eV)]\,\mathrm{d}E_{\perp}, \tag{1}$$

where the tunneling probability P depends on energy $E_{\perp}$ associated with the motion perpendicular to the barrier, $f(E)$ is the Fermi distribution function, and h is the Planck's constant. Summation over k gives the total contribution from all electronic states. In an 1D system, if we assume that the potential barrier under bias voltage V is given by

$$U(x) = \begin{cases} 0, & x < 0, \\ U_{\mathrm{o}} - \dfrac{eV}{d}x, & 0 \leqslant x \leqslant d, \\ -\,eV, & x > d \end{cases} \tag{2}$$

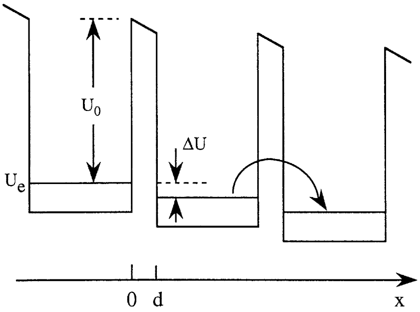

Fig. 7. Schematical description of potential barrier $U(x)$. $\Delta U = eV$ is the applied biased voltage, and d is the potential barrier width.

as shown in Fig. 7, where d is the width of the potential barrier. If $U_o \gg eV$, the tunneling probability P can be found by the WKB method,

$$P \approx U_o^{-1/4}\exp\left[-\frac{4\pi}{h}\int_0^d\sqrt{2m\left(U_o-\frac{eV}{d}x\right)}\,dx\right]$$
$$\approx U_o^{-1/4}\exp(-cd+\alpha V), \tag{3}$$

where c and α depends on the form of the potential barrier, and

$$\alpha = \frac{e}{2\hbar}\sqrt{\frac{2m}{U_o}}d. \tag{4}$$

Then the current has a form

$$I = a\frac{2e}{h}Ve^{-cd+\alpha V}, \tag{5}$$

where a is related to the density of states near the Fermi energy and the potential barrier. The system is Ohmic for small bias, and the current depends exponentially on V for large bias (comparable or larger than $1/\alpha$). In general, the shape of the potential barrier is not regular. However, we expect that the qualitative behavior should not change much, and one can still use these equations by defining an effective (averaged) potential barrier U_o.

The exponential exponent α can be experimentally measured. As mentioned in the previous section for Fig. 2, the I–V characteristic of an as-fabricated sample (state (a)) at room temperature gives $\alpha = 0.23$, and it equals to 0.15 when the sample was "annealed" under 20 V for 1 h to a stable state (state (f)). Using Eq. (4), the exponents can be used to estimate the average potential barrier U_o and the potential barrier width. In general, both of the potential barrier and effective electron mass depend on the state of the Te clusters. It is reasonable to assume that the electron effective mass is close to the free electron mass because Te atoms are expected to be loosely bound together when the cluster is in state (a) [9]. On the other hand, Te atoms are tightly bound together when the cluster is in state (f). One may expect that the effective electron mass approaches that in a bulk Te material which is $m^* = 0.05m_e$ [13]. This mass difference in states (a) and (f) can contribute to the change in α besides the contribution from the change in the width d and the potential barrier U_o. For $d_a = 1.3$ Å, $m_a = m_e$, and $m_f = 0.05m_e$, where subscripts indicate states (a) and (f), we find $U_o = 2.2$ eV from Eq. (4) for state (a). If one assumes that U_o is the same both in states (a) and (f), the barrier width in state (f) can be found from

$$d_f = d_a\frac{\alpha_f}{\alpha_a}\sqrt{\frac{m_a}{m_f}} = 3.8\,\text{Å}. \tag{6}$$

The value means that a Te cluster has been roughly compressed by a half Te atom under an external electric field. This estimation is consistent with our physical picture [9] that barrier width will increase. Of course, the assumption that U_o does not change cannot be correct. Similar to the Schottky barrier at a semiconductor interface, Te cluster structure may greatly change the U_o at a range to the order of Å. Also, the difference of effective electron mass in states (a) and (f) may not be as large as those used in above estimation. If we assume that the change in α is purely from the change in U_o, and the effective electron mass is chosen to be that of a free electron, then, keeping $d = 1.3$ Å,

$$U_f = U_a\left(\frac{\alpha_a}{\alpha_f}\right)^2. \tag{7}$$

Substituting $\alpha_a = 0.23$, $\alpha_f = 0.15$, and $U_a = 2.2$ eV, the barrier height in state (f) is 5.2 eV which is very reasonable. Obviously, the actual behavior of the system should be somewhere between the two extremes mentioned above.

3.2. Structure change and relaxation under an external electric field

So far, we are able to explain the exponential feature in I–V curve based on quantum tunneling. However, one needs extra physics to understand the occurrence of the hysteresis current loop and peak. From Eq. (4), one may phenomenologically attribute the observed I–V features to the history dependence of the potential barrier. It is plausible that the potential barrier will change when there is a change in the electronic or atomic structures of Te clusters. The response of an electron to an external force is usually very fast with a time scale much shorter than a second. It is unlikely that the hysteresis current loop is due to the direct change in the electronic structure. However, atoms and atom clusters are heavy, and their response to an external force would be slow. It is more natural to explain the observed I–V characteristics by the structure change of Te clusters under an applied electric field. In a zeolite LTA (shown in Fig. 1), Na^+ ions exist near the 6-rings in the sodalite-cage surfaces, facing the supercage. The dipole field of AlO_4^-–Na^+ at supercage surface points outward. Without any bias, Te atoms are expected to be uniformly adsorbed on the inner surface of a supercage because of the dipole field. Taking the radius of the supercage and the Te atom as 5.5 and 1.6 Å, respectively, the maximum number of Te atoms that can be adsorbed on the inner surface is 13. This is a reasonable value because the number of Te atoms has been known to be 16 in Na-FAU [14]. When an external electric field is applied on the sample, the voltage drops mainly inside the barrier layer. An exponential dependence of the current on the applied voltage is expected. However, Te atoms are also expected to rearrange themselves under an external electric field. Several factors can cause this rearrangement. The Na^+ ions may move under the external electric field and therefore change the internal cage field. The external field can polarize the Te atoms. The polarization causes Te atoms to move to one side of supercage because the dipole field of AlO_4^-–Na^+ at the supercage surface. The rearrangement results from Te atoms moving very slowly toward the field direction such that Te clusters change from structure A to structure B shown in Fig. 8. Structure A corresponds to Te atoms uniformly distributed inside a supercage while, in structure B, Te atoms shift to one side of a supercage, creating an extra empty space in the supercage.

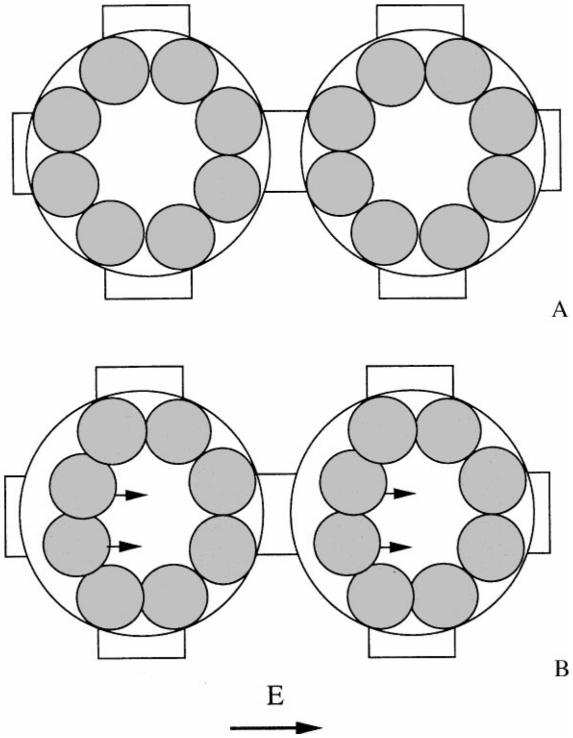

Fig. 8. Schematical drawing of Te cluster structures with and without an biased voltage. Te atoms are uniformly distributed in supercage in structure A which corresponds to the case in the absence of a biased voltage, and te atoms move to one side of supercage in structure B in a biased voltage.

The process that a Te cluster changes from structure A to B is very slow because of the tiny dipole–dipole interaction. In order to understand this slow dynamical process, it will be helpful to look at how the free energy change with the cluster structure. Without a biased voltage, structure A is a stable state while structure B becomes unstable. Schematically, we can plot the free energy surface of Te cluster against the so-called reaction coordinate Q. The left and right curves in Fig 9 are the free energies without and with an external electric field, respectively. Point A which denotes structure A is the minimum point of the left curve and point B which denotes structure B is the minimum point of

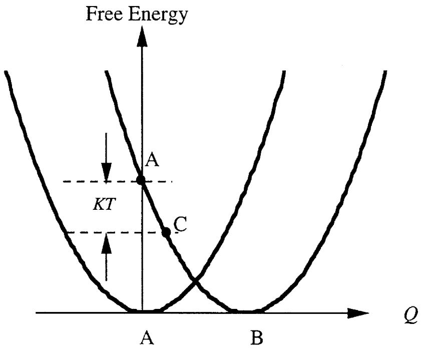

Fig. 9. The free energy surfaces of Te cluster without and with an external electric field, respectively. Points A and B correspond to structures A and B, respectively. In an external electric field, the energy difference between point A and point C′ is smaller than $3kT/2$.

the right curve. Applying an external field, structure A becomes unstable, and Te clusters will approach structure B along the right free energy curve in Fig. 9. The potential energy will be converted into kinetic energy on the way that structure A relaxes to structure B. The kinetic energy will be dissipated through Te–Te atom collisions. If p is the Te-atom dipole induced by an external electric field, and the mean distance of Te atoms is assumed to be the same as the mean free path l of the Te atoms, the average force between the two Te atoms is

$$f=\frac{6}{4\pi\varepsilon}\frac{p^2}{l^4}, \tag{8}$$

where ε is the permittivity. Then the typical velocity gained by a Te atom between two collisions can be estimated by

$$v_{\mathrm{d}}=\frac{f}{m}\frac{l}{v_{\mathrm{T}}}=\frac{3}{2\pi\varepsilon}\frac{p^2}{l^4 m}\frac{l}{v_{\mathrm{T}}}, \tag{9}$$

where v_{T} is the thermal velocity of a Te atom. In this very rough estimation, we consider only two Te atoms with dipole–dipole interaction, and the mean free collision time is approximated by l/v_{T}. If we let the polarizability of Te atoms be $10^{-24}\,(\mathrm{cm})^3$ in esu unit, $l = 1$ Å, $T = 300$ K, and the external electronic field strength be 10^5 V/m, then v_{d} is about 10^4 Å/s At finite temperature, there is a random kinetic energy to the order of $3kT/2$ for each Te atom. Therefore, when a Te cluster moves down on the free energy surface from A to C in Fig. 9, the cluster can still go back to A through the thermal motion. In order for the cluster to leave A irreversibly, an energy to the order of $3kT/2$ per Te atom on average must be taken away through collisions. In each collision, a kinetic energy to $Mv_{\mathrm{d}}^2/2$ per Te atom is dissipated, where M is the mass of a Te atom. Thus, the relaxation time of the cluster under an external electric field must approximately be

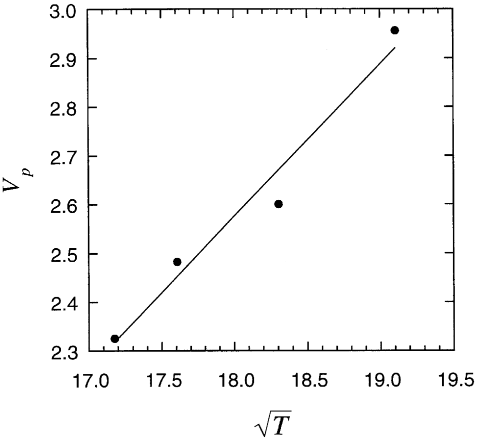

Fig. 10. The temperature dependence of the current peak positions. Dots are the experimental results and line is the square root of temperature fit.

$$\tau=\left(\frac{v_{\mathrm{T}}}{v_{\mathrm{d}}}\right)^2\frac{l}{v_{\mathrm{T}}}=\frac{v_{\mathrm{T}}}{v_{\mathrm{d}}^2}l\sim\sqrt{T}. \tag{10}$$

In other words, the relaxation time increases with the square root of temperature. If one associates the current peaks to the structure change of the Te clusters, the current peak position should be proportional to the relaxation time because the applied voltage increases linearly with time in our experiments. Therefore, the peak position should increase with $\sqrt{T}$, Fig. 10 is the temperature dependence of the peak position which agrees with $\sqrt{T}$. This explains the I–V curve (a) in Fig. 2. Namely, after certain time under an external electric field, Te atoms start to detach themselves from one side (against field direction) of the supercages. This detachment changes the shape of the potential barrier and increases the barrier width. Thus, the exponent α in Eq. (5) will decrease. This rearrangement of Te cluster will, therefore, cause the current drop which results in the current peaks observed. When the bias decreases, electrons need to tunnel through this new potential barrier. Therefore, current cannot follow its original path back. This is why we observed the current loops. As one repeats the measurement (keeping the bias direction unchanged), the clusters will gradually reach their stable state, and the loops will eventually disappear unless other means (such as applying a reverse bias, or thermally heating the sample) are adopted to return the clusters to their natural state (Te atoms being uniformly adsorbed on the inner surface of the supercages). For $T = 300\,\mathrm{K}$, $v_d = 10^4\,\mathrm{\AA/s}$, and $d = 1\,\mathrm{\AA}$, τ is in the order of 1 h. At least, the order of the time scale is correct in comparison with the experimental observations.

4. Discussion and summary

The reason that Te/LTA can undergo a structure change is that the Te atoms are loosely bound in a cluster. Such clusters are easy to be compressed. It is known that Te atoms are polarizable. The polarized Te atoms, in one hand, attract with each other due to the dipole–dipole interactions, and, on the other hand, be dragged to one side of the supercage surfaces because of the dipole and $\mathrm{AlO_4^-}$–$\mathrm{Na^+}$ dipole field interactions. Thus, an electric field can be used to compress the Te clusters. If this is true, we can use an electric field to control the fabrication of Te cluster solids in zeolite LTA. For example, one may use an electric field to control the number of Te atoms inside a supercage such that it may be possible to make the Te clusters so tight that their atomic structure cannot significantly change under an applied bias. It will be interesting to test this possible control mechanism.

We have studied the I–V characteristics of Te clusters in zeolite LTA. The Te clusters are expected to have the same size as the supercages. They are spatially confined and are isolated from each other. We believe that electrons move from one cluster to another mainly through quantum tunneling because the stable I–V curves are not very sensitive to temperature as shown in Fig. 5. An exponential dependence of the current on the applied voltage is expected. In order to explain the observed current loops and peaks in our experiments, we propose a Te atom rearrangement mechanism. As mentioned before, the Te-atoms span themselves from one side of the supercage to the other side in the absence of a biased voltage, forming structure A shown in Fig. 8. When an external electric field is applied on the sample, the Te atoms should move very slowly along the field direction, and they are expected to rearrange themselves to form structure B shown in Fig. 8. A Te cluster can change from structure A to B (Fig. 8) by dissipating extra energy through Te–Te atom collisions. Since there is a thermal motion, a cluster can dynamically have many different structures whose free energy differences are within the thermal energy $3kT/2$. If we assume that a cluster leaves its initial state only after it has dissipated an energy in the order of $3kT/2$, we may conclude that the relaxation time increases with temperature. When the electric field becomes strong and the drag force exerts on the Te atoms is long enough, the Te atoms will start to detach themselves from one side (against field direction) of the supercages as shown in Fig. 8(b). This detachment will cause a change of the potential barrier shape and an increase of the barrier width. This rearrangement of Te clusters will cause the current drop which gives the current peaks as observed. When the bias decreases, electrons need to tunnel through this new potential barrier. Therefore, current cannot follow its original path back. This is why we observed the current loops. As one repeats the measurement (keeping the bias direction unchanged), the clusters will gradually reach their stable state, structure B, and the loops will eventually disappear unless other means (such as applying a reverse bias, or thermally heating the sample) are adopted to return the clusters to their natural state, structure A (Te atoms being uniformly adsorbed on the inner surface of the supercages). In fact, we have seen that Te atoms have been dragged out of supercages when an constant external electric field is applied on a sample for a very long period of time (one day under 20 V in our sample). This observation strongly confirms the movement of Te atoms under an applied voltage. This picture is also consistent with our AC I–V measurements by applying a triangular voltage wave. Under low-frequency bias of 100 Hz, as shown in Fig. 6(a), the I–V curve is a non-monotonic function of voltage, showing a negative differential resistance region. When the frequency increases to 10 kHz, as shown in Fig. 6(b), a very symmetrical current wave is detected. In this case, the structure of the Te clusters cannot change substantially in a complete cycle (0.1 ms). Therefore, the potential barrier and thus the exponent α, do not change much so that no negative differential resistance appears at high frequency.

According to the above picture, the actual current loop should depend on how the I–V curve is measured. If the duration time of the applied constant voltage is changed, the loop should change too. If the duration time is so long that the Te clus ters have enough time to relax to its stable structure, then no current loop should be observed, and the I–V characteristics should be the same as that of curve (f) in Fig. 2. Indeed, when we changed the duration time from half a second to half an hour, the current loop disappeared and curve (f) in Fig. 2 was obtained. The above assumption also implies that the current peak (NDR) is a transient phenomenon.

In summary, we observed hysteresis current loops and current peaks in the I–V characteristics in a cluster superlattice of Te/LTA. The current peaks (NDR) do not result from the resonant tunneling transitions but are caused by a rearrangement of the Te atoms in the cluster. The observed I–V characteristics are transient in nature which depends on the sample temperature, the duration time of the applied voltage, etc. The temperature dependence of the current peak is consistent with the assumption that the transient nature is due to the fact that the Te atoms need to overcome their thermal motion in order to be rearranged.

Acknowledgements

This work was supported by UGC, Hong Kong, through DAG, RGC, and RTG grants.

References

[1] G.D. Stucky, J.E.M. Dougall, Science 247 (1990) 669.

[2] E.L. Shirley, L.X. Benedict, S.G. Louie, Phys. Rev. B 54 (1996) 10 970.

[3] R. Tsu, L. Esaki, Appl. Phys. Lett. 22 (1973) 562.

[4] L.L. Chang, L. Esaki, R. Tsu, Appl. Phys. Lett. 24 (1974) 593.

[5] L. Esaki, L.L. Chang, Phys. Rev. Lett. 33 (1974) 495.

[6] F. Capasso, K. Mohammed, A.Y. Cho, Appl. Phys. Lett. 48 (1986) 478.

[7] J.C. Jansen, M. Stocker, H.G. Karge, J. Weitkamp, (Eds.), Advanced Zeolite Science and Application, Elsevier, Amsterdam, 1994.

[8] V.N. Bogomolov, A.I. Zadorozhnyi, T.M. Pavlova, Sov. Phys. Semicond. 15 (1981) 1176.

[9] Z.K. Tang, X.R. Wang, Appl. Phys. Lett. 68 (1996) 3449.

[10] Y. Nozue, T. Kodaira, O. Terasaki, K. Yamazaki, T. Goto, D. Watanabe, J.M.W. Thomas, J. Phys.: Condens. Matter 2 (1990) 5209.

[11] Y. Nozue, Z.K. Tang, T. Goto, Solid State Commun. 73 (1990) 531.

[12] E. Cohen De Lara, R. Kahn, R. Seloudoux, J. Chem. Phys. 83 (1985) 2646.

[13] M. Lutz, H. Stolze, P. Grosse, Phys. Stat. Sol. B 62 (1974) 665.

[14] V.N. Bogomolov, A.I. Zadorozhnyi, T.M. Pavlova, V.P. Petranovskii, V.P. Podkhalyuzin, A.L. Kholkin, JETP Lett. 31 (1980) 378.